

## Chapter 10

# The Interaction of Single Beams of X and Gamma Rays with a Scattering Medium

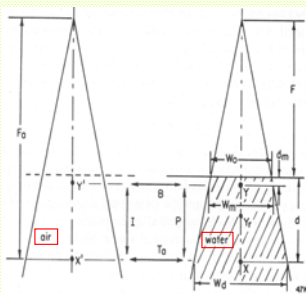
### Radiation Dosimetry I

Text: H.E Johns and J.R. Cunningham, The physics of radiology, 4<sup>th</sup> ed.  
<http://www.utoledo.edu/med/depts/radther>

## Dosimetric system

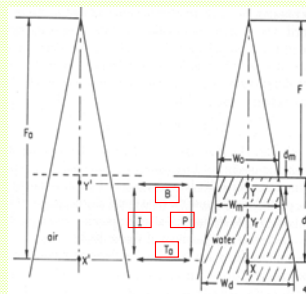
- Established a procedure for calculating dose at a point based on the measurement
- Now need to be able to calculate the dose at any point based on the known dose at the reference point
- A set of functions was developed to enable these calculations

## Parameters for calculation of absorbed dose



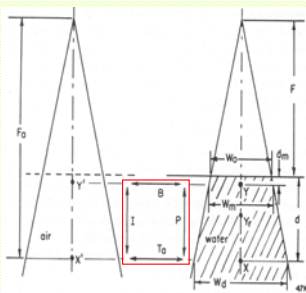
- Field width  $W$
- Distance from the source  $F$
- Depth in phantom  $d$
- Depth of the maximum dose in phantom  $d_m$
- Dose deposited at a certain point  $D_X, D_Y$ , etc.
- Dose is obtained under condition of electronic equilibrium (for air: enough phantom-like material surrounding the point)

## Functions used in dose calculation



- Tissue-air ratio  
 $T_a(d, W_d, hv) = D_X / D_{X'}$
- Backscatter factor  
 $B(W_m, hv) = T_a(d_m, W_m, hv) = D_Y / D_{Y'}$
- Percentage depth dose  
 $P(d, W_m, F, hv) = 100 D_X / D_Y$
- Inverse square law  
 $I(F, d, d_m) = \frac{D_{X'}}{D_{Y'}} = \left( \frac{F + d_m}{F + d} \right)^2$

## Relationship between functions



- Dose at one point can be calculated based on the known dose at a different point using a function along the corresponding arrow:

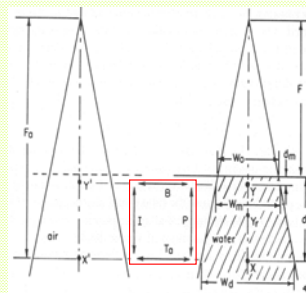
$$D_Y = D_{Y'} \cdot B$$

$$D_X = D_Y \cdot P$$

$$D_{X'} = D_{Y'} \cdot I$$

$$D_X = D_{X'} \cdot T_a$$

## Relationship between functions



- More than one function can be involved in relating doses at different points:

$$D_X = D_{Y'} \cdot B \cdot P$$

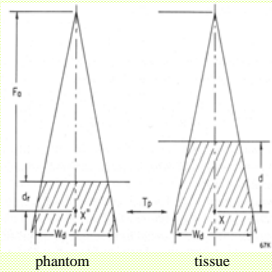
$$D_X = D_{Y'} \cdot I \cdot T_a$$

- Relationship between functions:

$$P(d, W_m, F) = \frac{100 \cdot T_a I}{B}$$

$$100 \frac{T_a(d, W_d) \left( \frac{F + d_m}{F + d} \right)^2}{B(W_m)}$$

## Tissue-phantom ratio



- For high-energy beams solid phantom is usually used for dosimetry
- Tissue-phantom ratio:

$$T_p(d, d_r, W_d, hv) = D_X / D_{X'}$$

- It can be related to  $T_a$ :

$$T_p = \frac{T_a(d, W_d, hv)}{T_a(d_r, W_d, hv)}$$

## Tissue-air ratio

- Introduced to simplify calculations for rotational therapy with tumor located at the rotational axis
- In such arrangement the source-to-axis distance is fixed
- For distances larger than 50 cm  $T_a$  is independent of the distance to the source (first determined experimentally)

## Tissue-air ratio

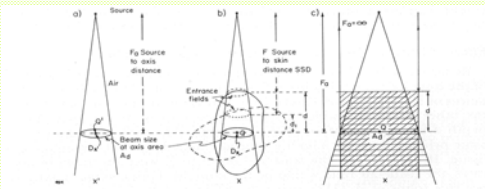
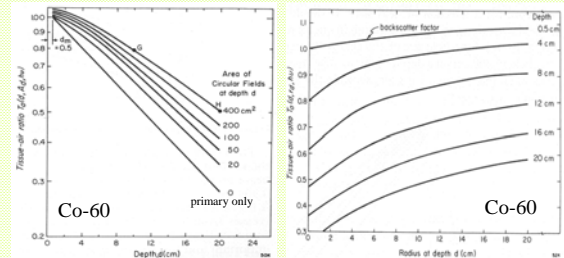


Figure 10-3. (a and b) Schematic diagram to illustrate the use of tissue-air ratio in dose calculations. (c) The scattering to point X from the cylindrical block of phantom material is the same as from the conical-shaped section when the two beams have the same area at depth d and receive the same primary radiation at X.

$$D_X = D_{X'} \cdot T_a(d, W_d, hv)$$

- $T_a$  values are tabulated for different field sizes, depths, and energies (Table B-5d)

## Tissue-air ratio



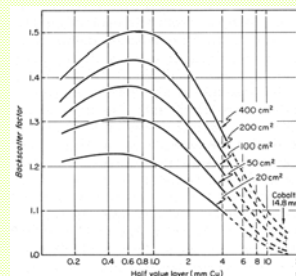
- Decreases almost exponentially with depth (Co-60 source is almost mono-energetic)
- Increases continuously with field size at all depth

## Backscatter factor

$$B(W_m, hv) = T_a(d_m, W_m, hv)$$

- Depends on the field size and quality of radiation
- Position of the maximum dose  $d_m$  depends on the field size and quality of radiation
- In general  $d_m$  is not the same as the depth where electronic equilibrium occurs: for large field sizes the scatter contribution determines the position of  $d_m$

## Backscatter factor



- The dependence on the radiation quality is non-monotonical, depends on field size
- For higher energies most of the scatter is forward-peaked: the amount of backscatter decreases

## Percentage depth dose

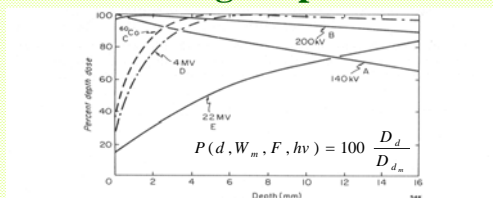


Figure 10-8. Percentage depth dose plotted against depth for the region near the surface for a range of photon beam energies.

- For higher energy beams there is a build-up region due to electrons scattered in forward direction
- After reaching its maximum dose deposition follows exponential attenuation

## Percentage depth dose

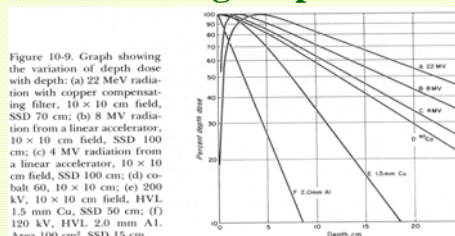


Figure 10-9. Graph showing the variation of depth dose with depth: (a) 2.2 MeV radiation with copper compensating filter, 10 × 10 cm field, SSD 70 cm; (b) 8 MV radiation from a linear accelerator, 10 × 10 cm field, SSD 100 cm; (c) 4 MV radiation from a linear accelerator, 10 × 10 cm field, SSD 100 cm; (d) cobalt 60, 10 × 10 cm; (e) 200 kV, 10 × 10 cm field, HVL 1.5 mm Cu, SSD 50 cm; (f) 120 kV, HVL 2.0 mm Al, Area 100 cm<sup>2</sup>, SSD 15 cm.

- After reaching its maximum dose deposition follows almost exponential decrease
- A useful quantity to use as an index of the penetration is the depth at which the dose falls to 50% of its peak value

## Percentage depth dose

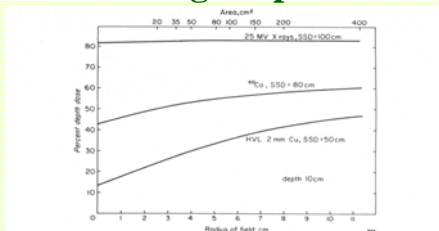


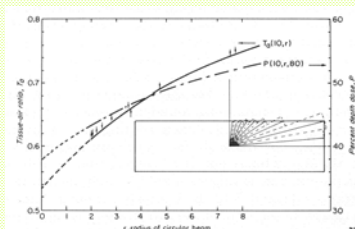
Figure 10-10. Variation of percentage depth dose with area and radius of field for three types of radiation. Depth 10 cm.

- For smaller field sizes scatter contribution is small
- For high energy beams scatter contribution is small, therefore PDD is less dependent on the field size

## Example 1

- All of the following are true regarding percentage depth dose (PDD) except:
    - A. Increases with increasing energy
    - B. Depends on field size
    - C. Is the dose at depth expressed as a percentage of the dose at  $d_m$
    - D. Decreases with increasing SSD
    - E. Decreases as depth increases
- ISL input decreases as distance increases through increase in SSD

## Equivalent field size



$$T_a(d, A) = \frac{1}{n} \sum_{i=1}^n T_a(d, r_i)$$

A – area of the field at depth d  
r – radius of the circular beam

- Rectangular field can be divided into segments of circular fields
- Functions ( $T_a$  or P) can be calculated for irregular field sizes
- Smaller angular segments increase the accuracy ( $10^\circ$  is typically enough)

## Equivalent field size

- A rectangular field gives a smaller depth dose and tissue-air ratio than does a circular or square field of the same area
- Rule of thumb method: Square fields and rectangular fields are equivalent if the ratios formed by dividing area by perimeter are the same ( $a/p$ )
- Tables 10.3 and 10.4 show radii of circular field and side length of square field corresponding to equivalent rectangular fields

## Equivalent field size

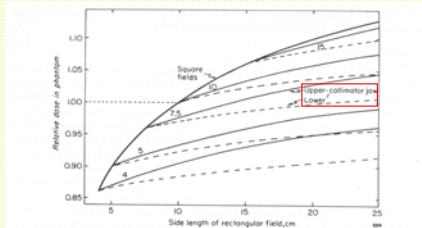


Figure 10-13. Relative output data for a 25 MV linear accelerator. The outputs were measured at a depth of 7 cm in a water phantom and are expressed as fractions of the output for a 10 x 10 cm field.

- In practice the output of the machine needs to be carefully measured for rectangular field sizes, due to the scatter from accelerator head

## Example 2

- A field measuring 5 x 25 cm at SSD has an "equivalent square" field of side \_\_\_\_ cm.

- A. 5.0
- B. 8.3**
- C. 11.2
- D. 16.1
- E. 25.0

$$\frac{a \cdot b}{2(a+b)} = \frac{c^2}{4c}$$

$$c = 2 \cdot \frac{a \cdot b}{a+b} = 2 \cdot \frac{5 \cdot 25}{5+25} = 8.3$$

## Dose profile

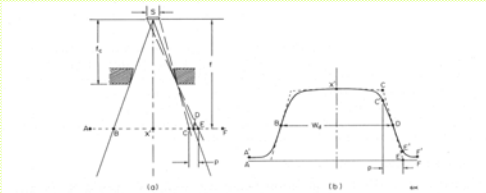


Figure 10-22. Diagrams illustrating properties of the primary component of a radiation beam. (a) The geometrical factors that lead to beam penumbra. (b) A dose profile as measured in air along the line A-F of a.

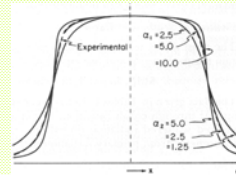
- Finite source size and beam shaping devices introduce geometric penumbra for primary radiation profile
- Scatter and flattening filter soften the edges of the beam

## Dose profile

- For field size (beam width) at depth  $d$ ,  $W_d$ , geometrical penumbra width  $p$ , the beam profile can describe by a function:

$$f(x) = 1 - 0.5 e^{-\alpha_1 p(|x| - W_d/2)} \text{ for } |x| \leq W_d/2$$

$$f(x) = t + (0.5 - t) e^{-\alpha_2 p(|x| - W_d/2)} \text{ for } |x| > W_d/2 \quad (10-16)$$



Parameters  $\alpha_1$ ,  $\alpha_2$ , and  $t$  are determined by best fit of measured profiles

## Dose profile

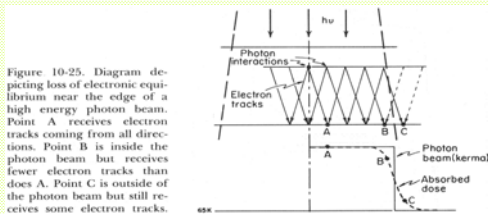


Figure 10-25. Diagram depicting loss of electronic equilibrium near the edge of a high energy photon beam. Point A receives electron tracks coming from all directions. Point B is inside the photon beam but receives fewer electron tracks than does A. Point C is outside of the photon beam but still receives some electron tracks.

- Even in the absence of scatter from beam shaping devices (primary collimator, jaws, etc.) the absorbed dose profile has a significant penumbra region
- Loss of lateral electronic equilibrium between kerma (energy lost by photons) and absorbed dose (energy lost by electrons)

## Description of the radiation beam

- Primary and scatter components: zero-field tissue-air ratio and scatter-air ratio

$$T_a(d, r_d, hv) = T_a(d, 0, hv) + S(d, r_d, hv)$$

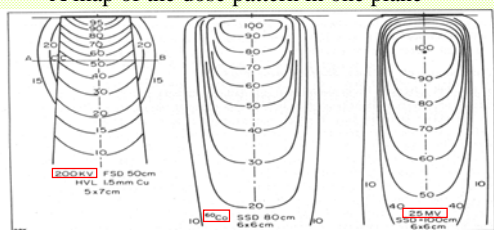
- For high-energy beams tissue-air ratio is replaced with tissue-phantom ratio

$$T_a(d, r_d, hv) = T_p(d, d_r, r_d, hv) \cdot T_a(d_r, r_d, hv)$$

- Due to relatively small amount of scattered radiation at high energies,  $T_a(d_r, r_d, hv) \sim 1$

## Isodose curves

- A map of the dose pattern in one plane



- No skin sparing, the dose falls continuously
- 25% at 10 cm depth
- Sharp beam edges
- Large amount of side scatter (beyond the beam)
- Skin sparing, the maximum at 5 mm
- 52% at 10 cm depth
- Penumbra
- Low side scatter
- Skin sparing, the maximum at 4 cm
- 83% at 10 cm depth
- Penumbra
- Low side scatter

## Example 3

- Compared with 6 MeV electrons, superficial x-rays:

- Have a lower skin dose
- Deliver less dose to underlying tissues
- Require thicker shielding
- Have a sharper penumbra

## Example 4

- In irregular field calculations, the increase in MU setting to account for blocking is greatest for:

- 18 MV photons, 12 cm depth
- 18 MV photons,  $d_m$
- 6 MV photons, 12 cm depth
- 6 MV photons,  $d_m$

Where the scatter contribution is the greatest: lower energy, greater depth

## Radiation beam characterization

- TG-106 report on accelerator beam commissioning: at a minimum, the following data should be collected during commissioning:
  - For photon beams—percent depth dose PDD and profiles in-plane and/or cross-plane at various depths for open and wedge fields, data related to multileaf collimator
  - MLC such as inter- and intraleaf leakage, penumbra, tongue and groove effect, etc., head collimator scatter, total scatter, tray, and wedge factors

L.J. Das, T. C. Zhu, et al. "Accelerator beam data commissioning equipment and procedures: Report of the TG-106 of the Therapy Physics Committee of the AAPM." Med. Phys. 35, 4186, 2008.

## Radiation beam characterization

- TG-21 report – protocol on clinical reference dosimetry, based on air kerma (obsolete)
- TG-51 report – protocol on clinical reference dosimetry, based on dose to water
- TG-40 report - protocol on comprehensive QA for medical linear accelerators
- TG-142 report - the most updated protocol on comprehensive QA for Radiation therapy, includes QA for on-board imaging and S(B)RT

P.R. Almond et al., "AAPM's TG-51 protocol for clinical reference dosimetry of high-energy photon and electron beams", Med. Phys. 26, 1847-1870, 1999.  
G. J. Kutcher et al., "Comprehensive QA for radiation oncology: Report of AAPM radiation therapy committee task group 40." Med. Phys. 21, 581-618, 1994.  
E.E. Klein, et al. "Task Group 142 report: Quality assurance of medical accelerators." Med. Phys. 36, 4197-4212, 2009.